Ink Removal in Whole Slide Images using Hallucinated Data

Vishwesh Ramanathan[ad], Wenchao Han[ad], Dina Bassiouny[bf], Eileen Rakovitch[ce], and Anne L. Martel[ad]

[a]Physical Sciences, Sunnybrook Research Institute, Toronto, Canada
[b]Department of Anatomic Pathology, Sunnybrook Health Sciences Centre, Toronto, Canada
[c]Department of Radiation Oncology, Sunnybrook Health Sciences Centre, Toronto, Canada
[d]Department of Medical Biophysics, University of Toronto, Canada
[e]Department of Radiation Oncology, University of Toronto, Canada
[f]Department of Pathology, Mansoura University, Mansoura, Egypt

ABSTRACT

Pathologists regularly use ink markings on histopathology slides to highlight specific areas of interest or orientation, making it an integral part of the workflow. Unfortunately, digitization of these ink-annotated slides hinders any computer-aided analyses, particularly deep learning algorithms, which require clean data free from artifacts. We propose a methodology that can identify and remove the ink markings for the purpose of computational analyses. We propose a two-stage network with a binary classifier for ink filtering and Pix2Pix for ink removal. We trained our network by artificially generating pseudo ink markings using only clean slides, requiring no manual annotation or curation of data. Furthermore, we demonstrate our algorithm's efficacy over an independent dataset of H&E stained breast carcinoma slides scanned before and after the removal of pen markings. Our quantitative analysis shows promising results, achieving 98.7% accuracy for the binary classifier. For Pix2Pix, we observed a 65.6% increase in structure similarity index, a 21.3% increase in peak signal-to-noise ratio, and a 30% increase in visual information fidelity. As only clean slides are required for training, the pipeline can be adapted to multiple colors of ink markings or new domains, making it easy to deploy over different sets of histopathology slides. Code and trained models are available at: https://github.com/Vishwesh4/Ink-WSI.

Keywords: Digital pathology, quality control, ink removal, classification, image-to-image translation, synthetic data

1. INTRODUCTION

The digitization of histopathology slides has ushered in the rise of computer-aided analyses and interpretation of histopathology images. Deep learning has emerged as the most popular technique for driving these computational analyses, and has been applied to address various problem spaces such as cell detection,[1,2] tissue segmentation,[3,4] cancer grading,[5] survival analysis[6,7] and much more.[8] However, these algorithms often require lots of clean, artifact-free data. In a clinical workflow, ink markings are introduced on histopathology slides as a medical record. These markings are often used to zone in on a specific area of interest, to identify regions of tissue to be sampled for further genetic sequencing, or in general, for correct orientation or guidance. Many pathologists routinely mark areas that may obscure important regions such as tumor stroma boundaries. These obscured regions carry lots of information such as immune cells response, etc, which may be useful for the downstream task. Unfortunately, the digitized version of these slides cannot be used for subsequent computational analysis due to the corruption of slides by ink markings. Subsequent cleaning and re-scanning of the slides double the workload of a pathologist and may potentially damage the slides. For downstream computational analyses, it is not only important to identify pen markings but also to successfully remove them. Hence, we require a methodology that could potentially identify and remove pen markings from whole slide images.

In this paper, we propose a methodology that could identify and remove the ink markings for the purpose of computational analysis without requiring any manually annotated or curation of data. We propose a two-stage network with a binary classifier for ink filtering and Pix2Pix for ink removal. We trained our network by artificially generating pseudo ink markings using only clean slides. This methodology removes the requirement

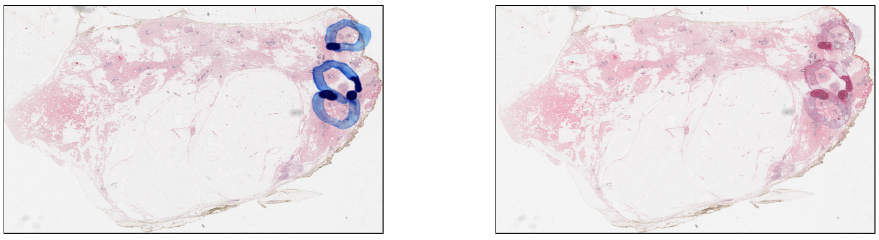

(a) Whole slide image with ink markings (b) Ink removal from proposed methodology.

Figure 1: Example of a whole slide image with ink markings, our goal is to remove the ink from the patches to enable computational analysis

of manually annotated data for training and makes it easier to expand the pipeline to new domains or multiple colors of ink markings. The efficacy of the methodology is evaluated based on multiple metrics such as accuracy, F1 score, structure similarity index (SSIM),[9] peak signal to noise ratio (PSNR)[10] and visual information fidelity (VIF),[11] over 45 pairs of ink stained and clean whole slide images.

2. RELATED WORKS

2.1 Image to Image translation

Image-to-image translation is a challenging problem in computer vision that aims to translate a given image from source domain X to target domain Y. In this paradigm, the domains X and Y share similar semantic structures but belong to different data distributions, for example, scans of the same body site using different modalities. In our study, we focus on Pix2Pix[12] model. It is a supervised method based on Conditional Generative Adversarial Networks or Conditional GANs,[13] which performs image-to-image translation by learning the mapping between the source(X) and the target domain(Y) using a corresponding dataset of images between X and Y domains. Pix2Pix, a Conditional GAN, has two different architectures for its generator and discriminator. For the generator, Pix2Pix uses U-Net,[14] an encoder-decoder type architecture primarily developed for medical image segmentation. The discriminator uses Patch-GAN, which classifies each $N \times N$ patch from the generator output as fake or real, and takes an average over all the predictions. The Pix2Pix network then uses a combination of L_1 and GAN loss to optimize its two networks. It has been widely used to tackle diverse problems in computational pathology. It has been used for stain normalization,[15] HE to immunofluorescence slide translation,[16] cytology segmentation,[17] high resolution image generation for data augmentation,[18] and many more.

2.2 Ink Removal

Several works have been proposed to address ink removal from histopathology images using image-to-image translation. Venkatesh et al.[19] used a Cycle GAN[20] for ink restoration given a set of ink patches. Cycle GANs, based on GANs[21] also do image-to-image translations by learning the mapping between source and target domain using unpaired dataset. However, directly using Cycle GANs introduces unrealistic hallucinations in some types of input patches.[22] To minimize this, Ali et al.[22] proposed a pipeline consisting of Convolutional Neural Network (CNN), You look only once (Yolov3)[23] and Cycle GAN to identify ink regions and subsequently remove them. In brief, using a Sequential CNN, the patches are classified into clean patches(tissue devoid of ink), ink patches (tissue containing ink), and patches with ink contaminating the background. Next, a Yolov3 was trained to get a precise location of ink-contaminated areas from the patch. Cycle GAN was then used to restore the ink inside the localized region and finally remove the ink markings. However, the pipeline faces many limitations. The workflow uses a combination of three algorithms. Errors at any intermediary steps will propagate to subsequent steps and magnify. Additionally, the pipeline requires a lot of well-annotated training data making the extension of the algorithm to different ink colors strenuous. To address some of these issues, Juang et al[24] introduced Pix2Pix[12] model for ink removal. The model is trained on patches from pairs of ink-stained and clean versions of the slides. For inference, all the patches (both ink and clean patches) are passed through the Pix2Pix model, which generates a clean version of the input patches. However, future expansion of the model to multiple ink markers would require pathologists to manually curate such a dataset by scanning slides with and without ink.

Additionally, the pipeline uses Pix2Pix on the clean patches, which may corrupt the information as it goes through the layers of conditional GANs.

3. METHODS

Our proposed methodology consists of two modules, a) Filter: a binary classifier with a Resnet18[25] backbone, and b) Corrector: a Pix2Pix architecture for removing ink from a given patch. In brief, patches of size $n \times n$ are extracted from a given whole slide image, which gets classified into clean or ink patches by the ink filter. All the ink patches are then passed to Pix2Pix, which generates a clean version of the ink patches. We curate the training dataset by artificially generating ink markings using image processing, given a clean set of patches for training the two modules. In the next subsection, we will discuss about artificially generating ink markings using the ink generation module in detail.

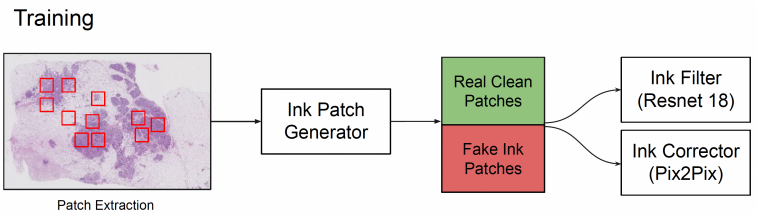

(a) Overview of the training pipeline

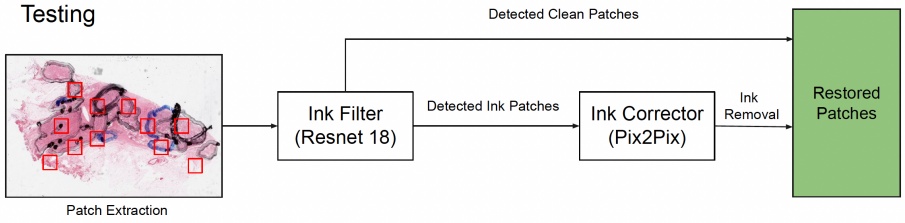

(b) Overview of the testing pipeline

Figure 2: Overview of the proposed methodology

3.1 Ink Patch Generation

To facilitate the training of models without any labels, we propose the generation of artificial ink markings given a clean patch using simple image processing techniques. Overall the ink mark in a patch can be broken down into three main components, 1) the pen blob, which may partially or fully cover the patch under consideration, 2) the color, 3) and the texture. To emulate these three components, our methodology consists of the following three steps, 1) generation of pen blob, 2) generation of colored texture, and 3) overlaying these two components onto the given clean patch. Figure 3 illustrates our ink patch generation algorithm.

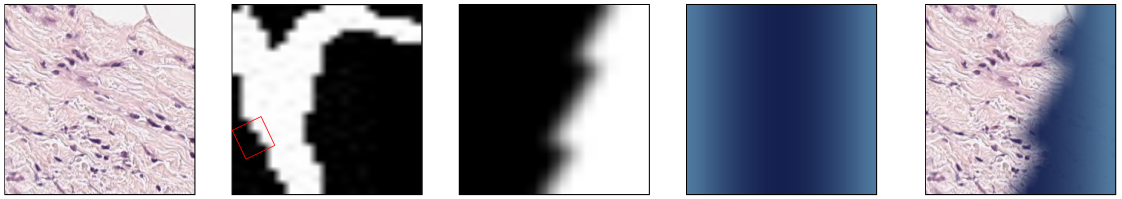

(a) Input clean patch

(b) Template image

(c) Generated pen blob from fig. 3b

(d) Generated colored texture

(e) Generated fake ink patch

Figure 3: Overview of ink patch generation using clean patch

3.1.1 Generation of Pen Blob

To mimic the streaks made by the pathologist, we use EMNIST,[26] an external handwritten dataset consisting of digits and English alphabets. We select an image from the dataset and extract a tile at a random location, angle, and scale. This way, we believe the extracted tile should emulate the shape of streaks that the pathologist would make at high magnifications. This would make the model robust against patches with partial ink coverings. Additionally, at random, we cover the whole patch with a pen blob to better replicate the diversity of ink markings in a patch. Using these steps, we generate a binary mask of the pen blob and resize it to the original patch size of $n \times n$. Finally, we smooth the edges of the pen blob by applying gaussian blur on the binary mask.

3.1.2 Generation of Colored Texture

Since the markers used to color the WSI may have some inconsistencies in the intensity of ink across its markings, we emulate this intricacy by taking color gradients across two random shades of a chosen ink color. We consider multiple gradient types, such as linear, gaussian, or no gradient, to capture different kinds of varying ink intensity inconsistencies. We also apply gaussian blur to get a smoother texture.

3.1.3 Overlaying

Let the given clean patch be $\mathbf{I}$ of shape $n \times n \times 3$. Let the generated pen blob mask be $\mathbf{M}$ of shape $n \times n$ and the colored texture be $\mathbf{T}$ of shape $n \times n \times 3$. Taking a random opacity value $\alpha \in [0.5, 1]$, we overlay $\mathbf{T}$ and $\mathbf{M}$, onto $\mathbf{I}$ using the following equation, ensuring smooth transition.

$$\mathbf{G}_{ij:} = max(1 - \mathbf{M}_{ij}, 1 - \alpha) \cdot \mathbf{I}_{ij:} + min(\mathbf{M}_{ij}, \alpha) \cdot \mathbf{T}_{ij:} \tag{1}$$

where $\mathbf{G}$ is our generated ink patch, which can be used for training our two networks.

4. EXPERIMENTS

4.1 Dataset Preparation

For our experiments, we used two different datasets for training and testing. For training our algorithm, we used only clean slides without any annotations. We extracted patches at a uniform stride from the TIGER dataset[27] which has been collected from various sources at a resolution of $0.5\mu m/pixel$. For evaluation of our algorithm, we curated the test set using 45 H&E stained breast carcinoma slides procured at the Sunnybrook Research Institute scanned at $0.5\mu m/pixel$, containing ink markings of multiple colors. For each slide, we manually annotated ink markings and clean regions for model evaluations. To evaluate the Pix2Pix model, these 45 slides were subsequently cleaned and scanned at a higher resolution of $0.25\mu m/pixel$. We extracted pairwise patches using registration from both the clean and ink marked WSIs for Pix2Pix model evaluation. For each pair of whole slide images, the non-rigid transformation matrix was determined by RANSAC[28] from feature points detected using SIFT.[29] The transformation matrix was subsequently used for pairwise patch extraction from clean and ink-marked whole slide images. The size of the image patch was set to 256×256, and the resolution was fixed to $0.5\mu m/pixel$, for both training and testing.

(a) Extracted patch from the ink marked slide

(b) Extracted patch using registration from the clean slide

Figure 4: Example of pairwise patch extraction from ink marked and clean slides

4.2 Model Training

We used 92719 clean patches extracted from the TIGER dataset for training the ink filter. The patches were selected randomly, and ink marks were generated on top of it. We used seven colors (black, brown, violet, light blue, royal blue, light green, and teal) to generate ink marks. The network was trained using Binary Cross Entropy loss and optimized using Adam optimizer with a learning rate of 0.001 for over 139 epochs.

We used over 52169 clean patches extracted from the TIGER dataset for training the Pix2Pix network. To prevent a significant domain shift between the training and testing set for Pix2Pix, we used an additional 34 clean slides scanned at the Sunnybrook Research Institute separate from the test set. We extracted 33546 clean patches from this additional dataset. These 85715 clean patches, paired with artificially generated ink patches were used for training. The implementation of Pix2Pix was taken from the public repository.[30] The network was trained using the same set of hyperparameters as the original paper.[12]

4.3 Evaluation

For quantitative evaluation of our networks, we evaluate our ink filter network based on F1 scores, Area under the Receiver Operation Characteristics curve(AUCROC), Recall, Accuracy, and Precision metrics. For the evaluation of ink removal using Pix2Pix, we utilize multiple image metrics such as PSNR,[10] SSIM,[9] and VIF,[11] giving an overall picture regarding the quality of ink removal. PSNR is the logarithm of division of the peak signal over mean squared error between the reference and target images, which gives an approximation of the restoration quality. SSIM, ranging from -1 to 1, calculates the degradation in structure between reference and target images, meanwhile also taking luminance and contrast differences into account. VIF emulates human perception of differences in the quality of images using concepts from information theory. For all these metrics, a high value indicates better restoration quality.

5. RESULTS

5.1 Ink Filter

Overall, for testing our ink filter, we extracted 71812 patches consisting of 28375 patches containing ink marks and 43437 clean patches with no ink marks, from the test set. The network achieved 98.73% accuracy on the test set as shown in table 1. Figure 5 illustrates a heatmap of classification using an ink filter. The heatmap demonstrates the efficacy of the network in detecting ink marks from WSIs.

Table 1: Performance of ink filter on testset

Total Patches	**True Positive**	**False Positive**	**False Negative**	**True Negative**
71812	27512	47	863	43390
Accuracy	**Precision**	**Recall**	**F1 Score**	**AUCROC**
98.73%	0.99	0.97	0.98	0.99

5.2 Ink Removal

For testing Pix2Pix for ink removal, we extracted 30000 pairs of patches from both sets of ink marked and clean slides. The patches extracted from the ink-marked set of slides consisted of 15000 ink and 15000 clean patches. For evaluating the algorithm, we calculated SSIM, PSNR, and VIF image metrics using pairs of patches across different data groups. The data was divided into four groups, *all tissue*, *inked tissue*, *clean tissue*, and *filtered tissue patches*. Here *clean patches* refer to 15000 clean patches that were passed through the Pix2Pix network to assess if the model degraded the quality. *Inked tissue patches* refers to 15000 ink patches that were passed through the Pix2Pix network. Here *all tissue patches* denotes all the 30000 patches in the test set, both ink and clean, that were passed to the Pix2Pix network. *Filtered tissue patches* denotes our pipeline where only patches that have been determined as ink patches by the ink filter network were passed to Pix2Pix, leaving the model-determined clean set of patches unchanged. The results of the experiments are shown in table 2.

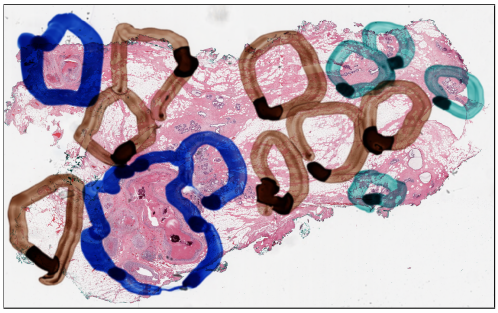

(a) Whole slide image with ink markings

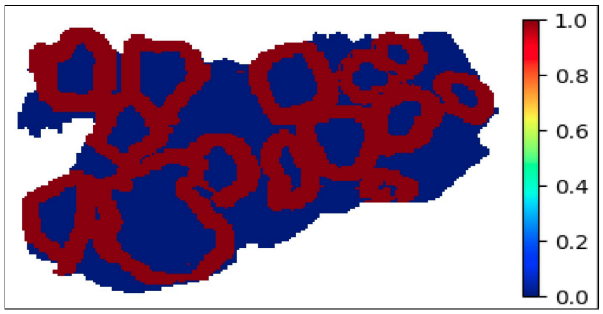

(b) Heatmap generated using ink filter. The red color denotes the detected ink patch and the blue color denotes the clean patch

Figure 5: Output of Ink Filter network. Each pixel in the map (b) corresponds to the output of the ink filter with 256×256 patch as the input, extracted at a uniform stride of 256 pixels

Table 2: Performance of Pix2Pix on 30000 patches from testset across different groups of data. Here *original* and *restored* refer to before and after patch restoration using Pix2Pix. Values are shown in the format of mean $\pm$ std

	SSIM		**PSNR**		**VIF**	
	Original	**Restored**	**Original**	**Restored**	**Original**	**Restored**
All tissue patches	0.32 $\pm$0.33	0.54 $\pm$0.19	13.51 $\pm$5.77	16.43 $\pm$3.97	0.10 $\pm$0.11	0.13 $\pm$0.11
Inked tissue patches	0.05 $\pm$0.22	0.47 $\pm$0.20	9.13 $\pm$4.10	14.95 $\pm$3.88	0.08 $\pm$0.14	0.14 $\pm$0.13
Clean tissue patches	0.59 $\pm$0.17	0.61 $\pm$0.16	17.88 $\pm$3.83	17.91 $\pm$3.48	0.12 $\pm$0.07	0.13 $\pm$0.07
Filtered tissue patches	0.32 $\pm$0.33	0.53 $\pm$0.20	13.51 $\pm$5.77	16.39 $\pm$3.94	0.10 $\pm$0.11	0.13 $\pm$0.11

We observe an increase in SSIM, PSNR and VIF by 65.6%, 21.3% and 30% for our methodology respectively, indicating improvement in image quality after restoration. For the *clean tissue patches* group, we observe the SSIM of the original group to be around 0.59 ± 0.17, suggesting a quality difference between slides scanned at $0.25\mu m/pixel$ (clean slides) and those scanned at $0.5\mu m/pixel$ (ink slides), even in areas devoid of ink markings. We can also visually observe the quality difference in Patch 3 column of Figure 6. We also observe an insignificant difference in the image metrics before and after restoration for the *clean tissue patches* group, which confirms that our Pix2Pix network is not degrading the clean set of patches.

We also showcase qualitative results of ink removal using Pix2Pix. Figure 6 showcases the successful restoration by the trained Pix2Pix model. We observe that our model has successfully restored patches with different ink colors, light ink shades, dark ink shades, and no ink shades. Our model however struggles with dark ink shades as shown in figure 7. From these patches, it isn't easy to retrieve the high frequency information, due to which we observe Pix2Pix generating synthetic textures as shown in *Patches 1, 4, and 5*. We also observe Pix2Pix adding colors to light regions present in the original patches with dark ink. Additionally, we observe that the color of the nuclei is not restored correctly for some patches. We also observe *Patch 1* in figure 7 to be restored differently as compared to *Patch 4* which is just as dark. This may potentially indicate different levels of performance of the Pix2Pix network for different ink colors.

6. CONCLUSION

In this work, we have presented a methodology for identifying and removing ink markings without requiring any curated or annotated data and using only clean slides. We trained the proposed pipeline consisting of ink filter (Resnet18) and Pix2Pix by using clean patches and artificially generated ink patches. We have demonstrated its efficacy by testing it successfully on whole slide images with real ink markings. The ink filter presented has a high F1 score, and the Pix2Pix network shows promising results with increased SSIM, PSNR, and VIF scores. This work addresses the limitations of strenuous data collection. This makes the expansion of the pipeline to new domains and multiple ink colors easier, opening the possibility of easier deployment to different sets of

histopathology slides. For future work, we plan to investigate further whether the discoloration of nuclei affects downstream tasks such as nuclei segmentation. We would also like to evaluate image metrics for the restoration of patches with different ink colors since the Pix2Pix network may particularly struggle with colors close to the eosin stain of pink.

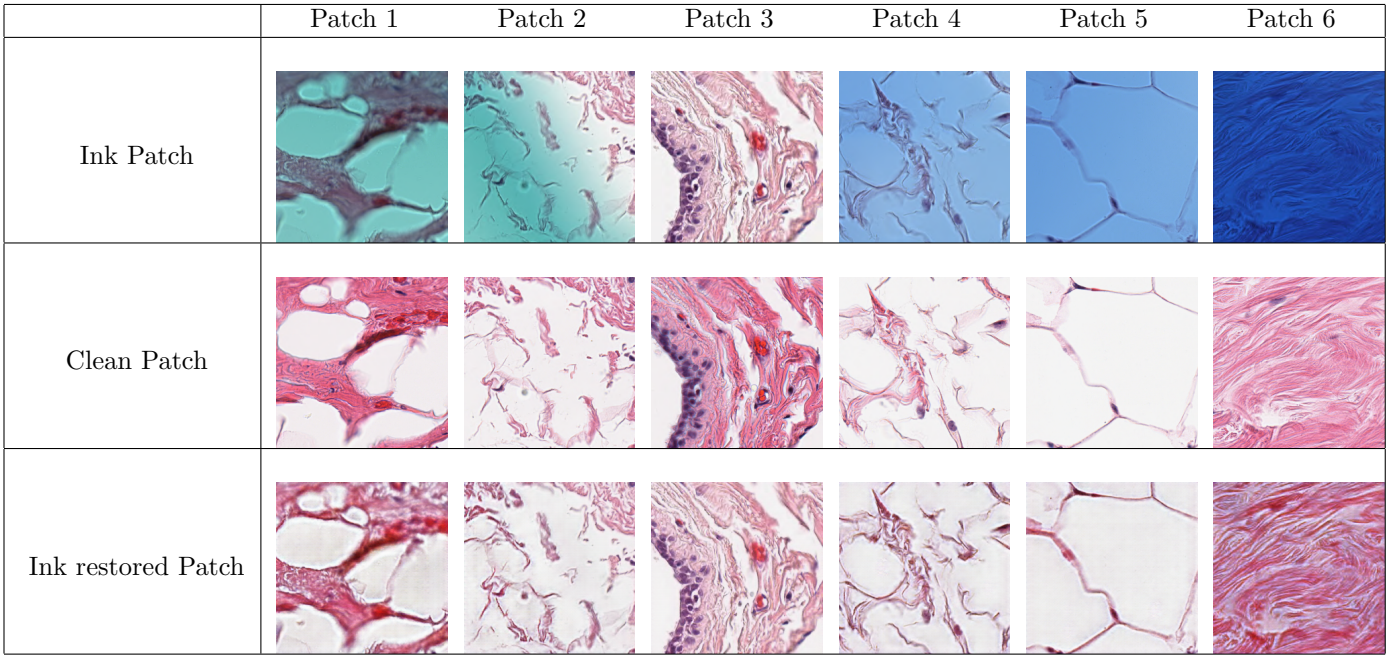

Figure 6: Patch restoration of different patches using Pix2Pix

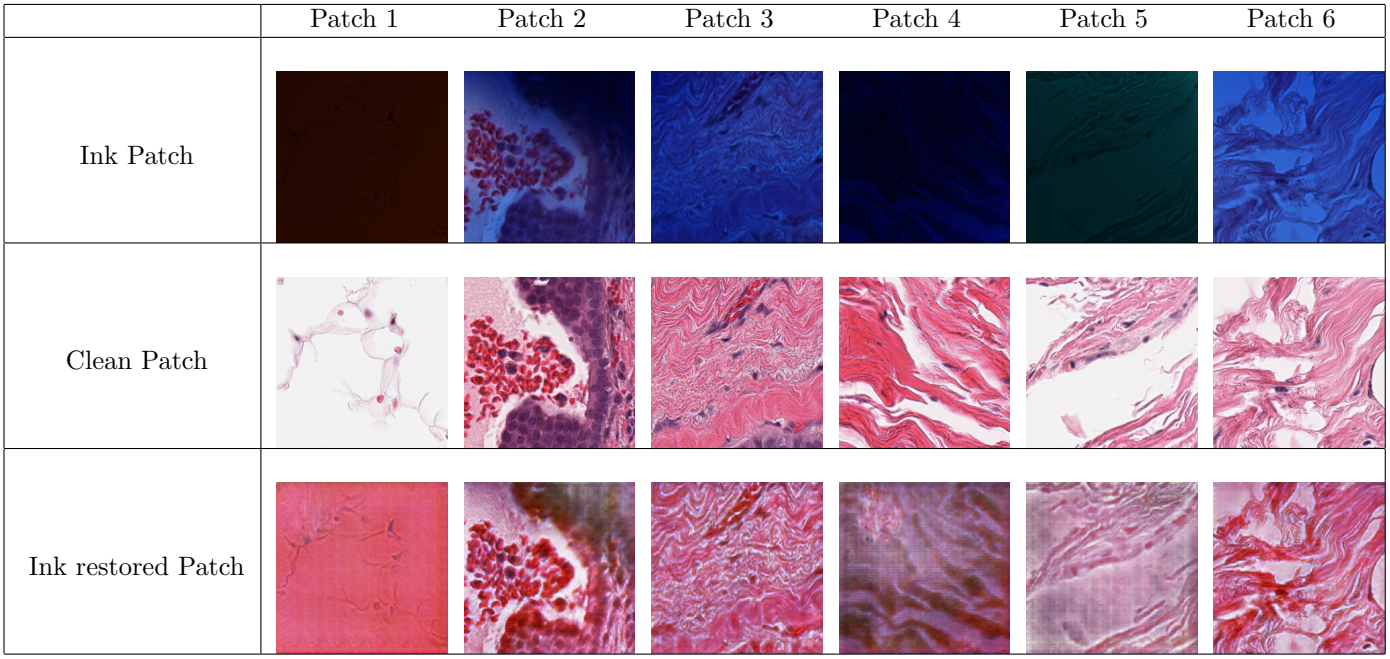

Figure 7: Failure cases of patch restoration using Pix2Pix

REFERENCES

[1] Graham, S., Vu, Q. D., Raza, S. E. A., Azam, A., Tsang, Y. W., Kwak, J. T., and Rajpoot, N., "Hover-net: Simultaneous segmentation and classification of nuclei in multi-tissue histology images," *Medical Image Analysis* **58**, 101563 (2019).

[2] Chen, T. and Chefd'Hotel, C., "Deep learning based automatic immune cell detection for immunohistochemistry images," in [*International workshop on machine learning in medical imaging*], 17–24, Springer (2014).

[3] Wang, J., MacKenzie, J. D., Ramachandran, R., and Chen, D. Z., "A deep learning approach for semantic segmentation in histology tissue images," in [*International Conference on Medical Image Computing and Computer-Assisted Intervention*], 176–184, Springer (2016).

[4] Qaiser, T., Tsang, Y.-W., Taniyama, D., Sakamoto, N., Nakane, K., Epstein, D., and Rajpoot, N., "Fast and accurate tumor segmentation of histology images using persistent homology and deep convolutional features," *Medical image analysis* **55**, 1–14 (2019).

[5] Ström, P., Kartasalo, K., Olsson, H., Solorzano, L., Delahunt, B., Berney, D. M., Bostwick, D. G., Evans, A. J., Grignon, D. J., Humphrey, P. A., et al., "Artificial intelligence for diagnosis and grading of prostate cancer in biopsies: a population-based, diagnostic study," *The Lancet Oncology* **21**(2), 222–232 (2020).

[6] Wulczyn, E., Steiner, D. F., Xu, Z., Sadhwani, A., Wang, H., Flament-Auvigne, I., Mermel, C. H., Chen, P.-H. C., Liu, Y., and Stumpe, M. C., "Deep learning-based survival prediction for multiple cancer types using histopathology images," *PloS one* **15**(6), e0233678 (2020).

[7] Li, R., Yao, J., Zhu, X., Li, Y., and Huang, J., "Graph cnn for survival analysis on whole slide pathological images," in [*International Conference on Medical Image Computing and Computer-Assisted Intervention*], 174–182, Springer (2018).

[8] Srinidhi, C. L., Ciga, O., and Martel, A. L., "Deep neural network models for computational histopathology: A survey," *Medical Image Analysis* **67**, 101813 (2021).

[9] Sheikh, H. R. and Bovik, A. C., "A visual information fidelity approach to video quality assessment," in [*The first international workshop on video processing and quality metrics for consumer electronics*], **7**(2), 2117–2128, sn (2005).

[10] Sara, U., Akter, M., and Uddin, M. S., "Image quality assessment through fsim, ssim, mse and psnr—a comparative study," *Journal of Computer and Communications* **7**(3), 8–18 (2019).

[11] Wang, Z., Bovik, A. C., Sheikh, H. R., and Simoncelli, E. P., "Image quality assessment: from error visibility to structural similarity," *IEEE transactions on image processing* **13**(4), 600–612 (2004).

[12] Isola, P., Zhu, J.-Y., Zhou, T., and Efros, A. A., "Image-to-image translation with conditional adversarial networks," in [*Computer Vision and Pattern Recognition (CVPR), 2017 IEEE Conference on*], (2017).

[13] Mirza, M. and Osindero, S., "Conditional generative adversarial nets," *arXiv preprint arXiv:1411.1784* (2014).

[14] Ronneberger, O., Fischer, P., and Brox, T., "U-net: Convolutional networks for biomedical image segmentation," in [*International Conference on Medical image computing and computer-assisted intervention*], 234–241, Springer (2015).

[15] Salehi, P. and Chalechale, A., "Pix2pix-based stain-to-stain translation: A solution for robust stain normalization in histopathology images analysis," in [*2020 International Conference on Machine Vision and Image Processing (MVIP)*], 1–7, IEEE (2020).

[16] Burlingame, E. A., Margolin, A. A., Gray, J. W., and Chang, Y. H., "Shift: speedy histopathological-to-immunofluorescent translation of whole slide images using conditional generative adversarial networks," in [*Medical Imaging 2018: Digital Pathology*], **10581**, 29–35, SPIE (2018).

[17] Levy, J. J., Jackson, C. R., Sriharan, A., Christensen, B. C., and Vaickus, L. J., "Preliminary evaluation of the utility of deep generative histopathology image translation at a mid-sized nci cancer center," *bioRxiv* (2020).

[18] Li, W., Li, J., Polson, J., Wang, Z., Speier, W., and Arnold, C., "High resolution histopathology image generation and segmentation through adversarial training," *Medical Image Analysis* **75**, 102251 (2022).

[19] Venkatesh, B., Shaht, T., Chen, A., and Ghafurian, S., "Restoration of marker occluded hematoxylin and eosin stained whole slide histology images using generative adversarial networks," in [*2020 IEEE 17th International Symposium on Biomedical Imaging (ISBI)*], 591–595, IEEE (2020).

[20] Zhu, J.-Y., Park, T., Isola, P., and Efros, A. A., "Unpaired image-to-image translation using cycle-consistent adversarial networks," in [*Proceedings of the IEEE International Conference on Computer Vision (ICCV)*], (Oct 2017).

[21] Goodfellow, I., Pouget-Abadie, J., Mirza, M., Xu, B., Warde-Farley, D., Ozair, S., Courville, A., and Bengio, Y., "Generative adversarial networks," *Communications of the ACM* **63**(11), 139–144 (2020).

[22] Ali, S., Alham, N. K., Verrill, C., and Rittscher, J., "Ink removal from histopathology whole slide images by combining classification, detection and image generation models," in [*2019 IEEE 16th International Symposium on Biomedical Imaging (ISBI 2019)*], 928–932, IEEE (2019).

[23] Redmon, J. and Farhadi, A., "Yolov3: An incremental improvement," *arXiv preprint arXiv:1804.02767* (2018).

[24] Jiang, J., Prodduturi, N., Chen, D., Gu, Q., Flotte, T., Feng, Q., and Hart, S., "Image-to-image translation for automatic ink removal in whole slide images," *Journal of Medical Imaging* **7**(5), 057502 (2020).

[25] He, K., Zhang, X., Ren, S., and Sun, J., "Deep residual learning for image recognition," in [*Proceedings of the IEEE conference on computer vision and pattern recognition*], 770–778 (2016).

[26] Cohen, G., Afshar, S., Tapson, J., and Van Schaik, A., "Emnist: Extending mnist to handwritten letters," in [*2017 international joint conference on neural networks (IJCNN)*], 2921–2926, IEEE (2017).

[27] Diagnostic Image Analysis Group, R. U. M. C., "Tiger grandchallenge official website." https://tiger.grand-challenge.org/Data/. (Accessed on 08/05/2022).

[28] Fischler, M. A. and Bolles, R. C., "Random sample consensus: a paradigm for model fitting with applications to image analysis and automated cartography," *Communications of the ACM* **24**(6), 381–395 (1981).

[29] Lowe, D. G., "Distinctive image features from scale-invariant keypoints," *International journal of computer vision* **60**(2), 91–110 (2004).

[30] Zhu, J.-Y. and Park, T., "Github code repository: pytorch-cyclegan-and-pix2pix: Image-to-image translation in pytorch." https://github.com/junyanz/pytorch-CycleGAN-and-pix2pix. (Accessed on 08/05/2022).